Hindawi
Advances in Materials Science and Engineering
Volume 2022, Article ID 3453797, 11 pages
https://doi.org/10.1155/2022/3453797

Research Article

Mesoscopic Fracture Model of Coarse Aggregate Interlocking Concrete

Ben Li,[1,2] **Ying Yu**,[2] **Chen Zhang**,[2] **and Yu Zhang**[2]

[1]*Opening Funding Supported by the Key Laboratory of Transport Industry of Road Structure and Material, (Research Institute of Highway Ministry of Transport), Beijing, China*
[2]*Advanced and Sustainable Infrastructure Materials Group, School of Transportation, Civil Engineering and Architecture, Foshan University, Foshan 528000, Guangdong, China*

Correspondence should be addressed to Ben Li; sktm1@163.com

Received 14 April 2022; Accepted 27 May 2022; Published 14 June 2022

Academic Editor: Xiaolong Sun

The skeleton formed by coarse aggregate has an important influence on the macroscopic mechanical properties of concrete, especially the fracture properties. Based on mesomechanics and fracture mechanics, this paper conducts theoretical simulations and experimental studies on the mechanical and fracture properties of coarse aggregate interlocking concrete through the theory of mesomechanics homogenization as well as compressive strength tests, flexural strength tests, axial compressive strength tests, elastic modulus tests, and fracture toughness tests. The results show that when the coarse aggregate is within a certain volume increase, the fracture energy and ultimate strength of concrete are significantly improved. At the same time, the proposed mesomechanics calculation model has high accuracy for calculating the fracture characteristics of concrete when the coarse aggregate increment is less than 20%.

1. Introduction

The mechanical strength and fracture toughness of concrete are material parameters that characterize the crack resistance and failure criteria of the material and are extremely important for the safe design of concrete members [1–3]. Concrete can be considered as a two-phase composite material containing mortar and aggregate [4–6], and its crack tips will form irregular intermittent cracks or crack extension zones during fracture. In recent years, relevant studies have shown that material property parameters such as fracture toughness and fracture energy of concrete are affected by significant size effects, and to obtain material parameters independent of the size of the concrete material, sufficiently large specimens must be cast [7–9]. In the concrete single-sided incised beam (SENB) specimen proposed by the International Federation for Research in Structures and Materials (RILEM) [5], the fracture parameters of concrete independent of size will not be obtained directly from this test because the concrete specimen size relative to the maximum particle size of the aggregate is not sufficiently large (W/dmax = 5~30). For this reason, revealing the effect of size on the fracture performance of concrete has become a hot spot for domestic and international research.

Cement paste forms a large component in conventional concrete, while the coarse aggregate content is very small. Coarse aggregates are the strength framework of concrete and are usually the strongest, most durable, and volumetrically stable structural units of concrete materials [10, 11]. As a composite material, the mechanical properties of the aggregate improve with increasing aggregate volume fraction as long as the aggregate is well integrated with the cement paste [12–14]. However, the mechanical behavior of concrete is not an absolute property and it is influenced by many factors. Traditional concrete has some problems in its mechanical design [15–17]: (1) The large amount of cement and cementitious materials leads to significant cracks in the concrete at an early stage, which in turn affects its mechanical and durability properties at a later stage. (2) The

low- or high-volume content of coarse aggregates not only fails to give full play to the strength contribution of aggregates but also causes adverse effects such as increased concrete cost, waste of resources, and increased environmental load. (3) In the process of concrete fracture, the initial crack tip between the aggregate and the cementitious material fails the cementitious occlusion leading to crack expansion. Therefore, the content of coarse aggregates in concrete will directly affect the mechanical properties of concrete. Hillerborg [18] proposed earlier that the development of the fracture process zone (FPZ) of concrete is essential in the development of aggregate bond bite cracking and proposed a virtual cracking model, which was widely used and became the basis for the study of quasi-brittle fracture of concrete. The influence of aggregate content on fracture energy and fracture process zone was analyzed; Zollinger et al. [19] showed through tests that the FPZ will increase with the increase in average aggregate size during concrete fracture. Currently, many studies have been conducted to construct high-performance, high-volume stability aggregate interlocking concrete by increasing the amount of coarse aggregates in order to greatly optimize the comprehensive performance and application of concrete materials [20, 21].

Among them, cast-in-place aggregate concrete, a newly proposed and promising coarse aggregate interlocking concrete, is considered as a new component to improve the service life of concrete by maximizing the material performance and reducing the incidence of diseases [22, 23]. Compared with conventional concrete, aggregate interlocking concrete has some significant advantages in terms of mechanical, durability, and stability properties [24–27]. In addition, the establishment of fracture models for aggregate interlocking concrete is basically based on three-point loading tests, and equally important mechanical tests such as compressive strength and modulus of elasticity and their mechanical mechanisms, especially fracture theory, have not been systematically studied. Fracture or cracking characteristics are the most required engineering and material properties of concrete, which are necessary signs to ensure the stability of concrete. Also, based on the influence of coarse aggregates, the internal nanostructure and hydration products of aggregate interlocking concrete are redistributed. Traditional mechanical models are not comprehensive in characterizing its fracture mechanism, and a multiscale model is needed for theoretical analysis.

Based on these backgrounds, the main objective of this paper is to investigate the fracture mechanism and theoretical calculation model of aggregate interlocking concrete. Based on the integration of fine-scale mechanics and fine-scale structural changes of concrete, a fine-scale transport model based on description, theoretical calculation, and numerical analysis is established and determined and its reliability is verified by macroscopic mechanical tests to provide a theoretical supplement and support for the mechanical mechanism of aggregate interlocking concrete.

2. Theoretical Analysis

The theory of fracture and damage of traditional concrete materials is established based on the energy law, crack development law, and other factors. However, it does not consider the changes in mechanical response caused by the increase in coarse aggregate and the interlocking shape. Considering the influence of coarse aggregate on the microstructure of concrete interface, a new fracture mechanism of aggregate interlocking concrete based on the theory of mesomechanics homogenization (RVE model) was established.

2.1. The RVE Model of Coarse Aggregate Interlocking Concrete. Suppose there is an elastic solid with a volume of V in the concrete matrix at the mesoscale and an inclusion subdomain in the inclusion and disturbance caused by coarse aggregate in elastic solids. The base domain and the inclusion domain have different elastic tensors and flexibility tensors. The inhomogeneity caused by the existence of pore structure inclusions due to the interaction of coarse aggregates will produce stress and strain field disturbances in a uniform solid. Therefore, the stress and strain equations of an elastic solid with pore structure inclusions can be expressed as

$$\begin{aligned} \sigma(X,x) &= \sigma^0(X) + \sigma^d(x), \\ \varepsilon(X,x) &= \varepsilon^0(X) + \varepsilon^d(x), \end{aligned} \tag{1}$$

where $\sigma(X,x)$ is the stress of a cement-based elastic solid with pore structure inclusions, $\varepsilon(X,x)$ is the strain of a cement-based elastic solid with pore structure inclusions, $\sigma^0(X)$ is the stress of the cement-based elastic solid, $\varepsilon^0(X)$ is the strain of the cement-based elastic solid, $\sigma^d(x)$ is the disturbance stress of the pore structure with inhomogeneous bodies, and $\varepsilon^d(x)$ is the disturbance strain of the pore structure with inhomogeneous bodies.

Through the superposition of the characteristic strain field and the actual strain field, the relationship between the equivalent uniform solid stress field and the original nonuniform stress field can be obtained:

$$\begin{aligned} \sigma(X,x) &= \mathbb{C}\colon \left[\varepsilon(X) - \varepsilon^*(x)\right], \\ &= \begin{cases} \mathbb{C}\colon \left[\varepsilon^0(X) + \varepsilon^d(x)\right] & x, X \subset M, \\ \mathbb{C}\colon \left[\varepsilon^0(X) + \varepsilon^d(x) - \varepsilon^*(x)\right] & x, X \subset \Omega, \end{cases} \end{aligned} \tag{2}$$

where $\mathbb{C}$ is the elasticity tensor of nonuniform solids, $\varepsilon^*(x)$ is the characteristic strain for simulating material mismatch, defect, pore structure, or inhomogeneity mismatch, M is the characteristic domain at the mesoscale of solids, and Ω is the inclusion subdomains in solids.

Therefore, the characteristic stress field of the pore structure in the hardened concrete due to the interaction of the coarse aggregate can be obtained:

$$\sigma^*_{\text{pore}}(x) = \mathbb{C}^I : \left[\varepsilon^*_{ij}(x)\right]_{\text{pore}} = \mathbb{C}^I : \left[\varepsilon^0(X) + \varepsilon^d(x)\right] - \sigma(X, x), \tag{3}$$

where $\mathbb{C}^I$ is the elastic tensor of the inclusion field.

In an infinite space, the induced displacement field caused by the characteristic strain field in the hole structure is determined as

$$\begin{aligned}\left[u_i(x)\right]^{\text{pore}} &= -\int_{\mathbb{R}^3} C_{jlmn}\varepsilon^*_{mn}(y)G^{\infty}_{ij,l}(x-y)d\Omega_y,\\ &= -\varepsilon^*_{mn}\int_{\Omega} C_{jlmn}G^{\infty}_{ij,l}(x-y)d\Omega_y,\\ &= \frac{\varepsilon^*_{mn}}{8\pi(1-\nu)}\left\{\frac{\partial^3\psi}{\partial x_i\partial x_m\partial x_n}\right.\\ &\quad \left. - 2(1-\nu)\left[\delta_{mi}\frac{\partial\phi}{\partial x_n} + \delta_{ni}\frac{\partial\phi}{\partial x_m}\right] - 2\nu\delta_{mn}\frac{\partial\phi}{\partial x_i}\right\},\end{aligned} \tag{4}$$

where $[u_i(x)]^{\text{pore}}$ is the induced displacement field caused by characteristic strain, $C_{\text{jlmn}}G^{\infty}_{ij,l}(x-y)$ is the Green transformation formula, and $\mathbb{R}^3$ is the unlimited space domain.

For the coarse aggregate lock concrete, the elastic strain field can be expressed as

$$\begin{aligned}\varepsilon_{ij}(x) &= \left\{\frac{1}{2}\left[u_{i,j}(x) + u_{j,i}(x)\right]\right\}\\ &= \frac{\varepsilon^*(x)}{8\pi(1-\nu)}\left[\psi_{,mnij} - 2\nu\delta_{mn}\phi_{,ij}\right.\\ &\quad \left. - (1-\nu)\left(\delta_{mi}\phi_{,nj} + \delta_{ni}\phi_{,mj} + \delta_{mj}\phi_{,ni} + \delta_{nj}\phi_{,mi}\right)\right].\end{aligned} \tag{5}$$

2.2. The Elastic-Plastic Constitutive Relationship of Aggregate Interlocking Concrete. According to Hooke's law, the relationship between elastic strain and Cauchy stress is

$$\begin{aligned}\sigma'_{ij}(x) &= C^{\text{concrete}}_{\text{ijkl}}\varepsilon^{*concrete}_{ij}(x)\\ &\quad + C_{ijkl}\left(\varepsilon^{*\text{concrete}}_{ij}(x) - \left[\varepsilon^*_{ij}(x)\right]_{\text{pore}} - \left[\varepsilon_{ij}(x)\right]^{\text{pore}}\right),\\ &= C^{\text{concrete}}_{\text{ijkl}}u^{\text{concrete}}_{i,j}(x)\\ &\quad + C_{ijkl}\left(u^{\text{concrete}}_{i,j}(x) - \left[\varepsilon^*_{ij}(x)\right]_{\text{pore}} - \left[\varepsilon_{ij}(x)\right]^{\text{pore}}\right).\end{aligned} \tag{6}$$

The theoretical solution of the elastic-plastic constitutive relationship of coarse aggregate lock-type concrete is determined as

$$\left[\sigma_{FAC}\right]_{ij} = \sigma'_{ij}(x) = \underbrace{\left[\overline{C_{FAC}}\right]_{ijkl}\otimes\left[\varepsilon_{FAC}\right]^{kl}}_{\text{elastic}} + \underbrace{\left[\overline{C_{FAC}}'\right]_{ijkl}\otimes\left[\varepsilon_{FAC}\right]'^{kl}}_{\text{plastic}}, \tag{7}$$

where $[\overline{C_{FAC}}]_{ijkl}$ is the effective modulus of the concrete in the elastic stage, $[\overline{C_{FAC}}']_{ijkl}$ is the effective modulus of the concrete in the plastic stage, $[\varepsilon_{FAC}]^{kl}$ and $[\varepsilon_{FAC}]'^{kl}$ is the strain of concrete in the elastic-plastic stage, and $[\sigma_{FAC}]_{ij}$ is the loading stress.

The effective modulus of concrete in the elastic stage is deduced based on the theory of generalized self-consistent method, which is the mechanical behaviour influenced by the interlocking of coarse aggregate and the mortar between the interface:

$$\begin{aligned}C^{pq}_{FAC} &= \left[1 + \frac{16}{9}\frac{1-\vartheta_1^2}{1-2\vartheta}f\left(V_{\text{Coarse aggregate interlocking}}\right) + \frac{4.35 - 2.06(1+\vartheta_1)}{1-2\vartheta}f^{2/5}\left(V_{\text{Coarse aggregate interlocking}}\right)\right]C^{pq}_{f\left(V_{\text{Coarse aggregate interlocking}}\right)}\\ &\quad + \left[1 + \frac{16}{9}\frac{1-\vartheta_2^2}{1-2\vartheta}f\left(\phi_{\text{pore}}\right) + \frac{4.35 - 2.06(1+\vartheta_2)}{1-2\vartheta}f^{2/5}\left(\phi_{\text{pore}}\right)\right]C^{pq}_{ITZ},\end{aligned} \tag{8}$$

where C^{pq}_{FAC} is the effective modulus of concrete, $C^{pq}_{f(V_{\text{Coarse aggregate interlocking}})}$ is the modulus of coarse aggregate under the interlocking action, $C^{pq}{}_{\text{ITZ}}$ is the modulus of ITZ, ϑ_1 is Poisson's ratio of coarse aggregate under the interlocking action, ϑ_2 is Poisson's ratio of ITZ, $f(V_{\text{Coarse aggregate interlocking}})$ is the density distribution of coarse aggregate, and $f(\phi_{\text{pore}})$ is the distribution characterization function of pore structure.

2.3. The Fracture Toughness Equation of Aggregate Interlocking Concrete. The fracture process of materials is predicted by the yield function during the plastic development.

Therefore, the fracture yield equation of concrete is established based on the Gurson model as

$$\Phi\left(\sigma_{ij}'(x),\sigma_e,f^*\left(\phi_{\text{pore}}\right)\right)=\left(\frac{\sum_{eq}}{\sigma_e}\right)^2+2f^*\left(\phi_{\text{pore}}\right)\cosh\frac{\overline{C_{FAC}}\cdot\overline{\overline{C_{FAC}'}}}{\overline{C_{FAC}}-\overline{C_{FAC}'}}\left(\frac{3\sum_m}{2\sigma_e}\right)-1-f^*\left(\phi_{\text{pore}}\right)^2=0,$$

$$f^*\left(\phi_{\text{pore}}\right)=f_c\left(\phi_{\text{pore}}\right)+\frac{0.53-f_c\left(\phi_{\text{pore}}\right)}{f_{fra}\left(\phi_{\text{pore}}\right)-f_c\left(\phi_{\text{pore}}\right)}\left(f\left(\phi_{\text{pore}}\right)-f_c\left(\phi_{\text{pore}}\right)\right),$$

$$\begin{aligned}\overline{C_{FAC}^{pq'}}&=\left[1+\frac{16}{9}\frac{1-\vartheta^2}{1-2\vartheta}f\left(V_{\text{Coarse aggregate interlocking}}\right)+\frac{4.35-2.06(1+t\vartheta)}{1-2\vartheta}f^{2/5}\left(V_{\text{Coarse aggregate interlocking}}\right)\right]C^{pq}_{f\left(V_{\text{Coarse aggregate interlocking}}\right)}+\\&\quad(1-D')\left[1+\frac{16}{9}\frac{1-\vartheta^2}{1-2\vartheta}f^*\left(\phi_{\text{pore}}\right)+\frac{4.35-2.06(1+t\vartheta)}{1-2\vartheta}f^{*,2/5}\left(\phi_{\text{pore}}\right)\right]C^{pq}_{ITZ}\\&=\left[1+\frac{16}{9}\frac{1-\vartheta^2}{1-2\vartheta}f\left(V_{\text{Coarse aggregate interlocking}}\right)+\frac{4.35-2.06(1+\vartheta)}{1-2\vartheta}f^{2/5}\left(V_{\text{Coarse aggregate interlocking}}\right)\right]C^{pq}_{f\left(V_{\text{Coarse aggregate interlocking}}\right)}\\&\quad+\left(1-\frac{\Delta R}{R_N}\right)\left[1+\frac{16}{9}\frac{1-\vartheta^2}{1-2\vartheta}f^*\left(\phi_{\text{pore}}\right)+\frac{4.35-2.06(1+t\vartheta)}{1-2\vartheta}f^{*,2/5}\left(\phi_{\text{pore}}\right)\right]C^{pq}_{ITZ},\end{aligned}\tag{9}$$

where $\Phi(\sum_{ij},\sigma_e,f^*(\phi_{\text{pore}}))$ is the yield function of concrete, $\sigma_{ij}'(x)$ is the macroscopic stress, σ_e is the equivalent yield stress, $\sum_{eq}$ is the Mises yield stress, $\sum_m$ is the hydrostatic stress, $f^*(\phi_{\text{pore}})$ is the porosity distribution function of the ITZ during the yielding process, $f_c(\phi_{\text{pore}})$ is the porosity distribution function when pore confluence begins, $f_{fra}(\phi_{\text{pore}})$ is the critical porosity distribution function when the material fractures, D' is the damage factor under load, ΔR is the pore size change value of ITZ, and R_N is the pore size characteristic value of ITZ.

Based on the fracture criterion, the fracture toughness equation of the coarse aggregate lock concrete is determined as

$$\widetilde{G}_{FAC}=\frac{2\pi(\sigma_e)^2}{\overline{C_{FAC}^{pq'}}},\tag{10}$$

where $\widetilde{G}_{FAC}$ is the fracture toughness of coarse aggregate interlocking concrete.

3. Experimental Details

3.1. Raw Materials and Mixing Proportions. Raw materials including local ordinary Portland cement of grade P.O 42.5 N from Guangzhou Yuebao Cement Co., local river sand with a fineness modulus of 2.3, and water were used throughout the study. Local limestone was used as a coarse aggregate, with a size ranging from 5 mm to 25 mm. Tables 1 and 2 show the mechanical and chemical properties of ordinary Portland cement. The physical properties of the river sand and coarse aggregates are presented in Table 3. In this experiment, the water-to-cement ratio (w/c) was 0.45, and the mixing proportion of concrete is shown in Table 4 (coarse aggregates increase by 5%, 10%, 15%, 20%, and 25% according to the volume percentage of the basic aggregate).

3.2. Specimen Casting and Curing Conditions. The concrete specimens were prepared in accordance with Chinese standard JTG 3420-2020 [28]. The dimensions of the concrete specimens were 150 mm × 150 mm × 150 mm (144 pieces), 100 mm × 100 mm × 400 mm (108 pieces), and 150 mm × 150 mm × 300 mm (108 pieces), and the specimens were demolded after 24 h. Each sample was placed in saturated limewater to cure at room temperature (i.e., 20 ± 2°C/RH ≥ 95%) for 28 days in accordance with GB/T50081-2019 [29].

3.3. Experimental Methods

3.3.1. Test Method for Strength of the Coarse Aggregate Interlocking Concrete. 150 mm × 150 mm × 150 mm (144 pieces) specimens were used for the compressive strength test, 100 mm × 100 mm × 400 mm (108 pieces) were used for the flexural strength test, and 150 mm × 150 mm × 300 mm (108 pieces) were used for the axial compressive strength test for 28 days according to GB/T50081-2019 [29].

3.3.2. Test of Elastic Modulus of the Coarse Aggregate Interlocking Concrete. The secant modulus under 30% axial compressive strength stress is taken as the elastic modulus value according to GB/T50081-2019 [29]. The size of the experimentally produced specimen is 150 mm × 150 mm × 300 mm (108 pieces).

Table 1: Mechanical properties of Portland cement (MPa).

Flexural strength (MPa)		Compressive strength (MPa)		Fineness	Setting time (h: m)	
3 days	28 days	3 days	28 days	1.8	Initial setting	Final setting
5.2	7.1	22.1	51.8		0 : 46	1 : 33

Table 2: Chemical properties of Portland cement (%).

Chemical component	Weight (%)	Chemical component	Weight (%)
SiO_2	21.50	TiO_2	0.23
Al_2O_3	4.50	Na_2O	0.33
Fe_2O_3	3	K_2O	0.39
CaO	65.70	SO_3	2
MgO	1.30	P_20_5	0.27
MnO	0.14	Cl	0.01

Table 3: Physical properties of the aggregates.

Physical properties	Fine aggregate	Coarse aggregate
Type	Natural stand	Crushed stone
Size (mm)	0.16–2.5	5–20.5
Apparent density (kg/m^3)	2,540	2,590
24-hour water absorption (%)	3.06	2.17
Fineness modulus	2.37	——

Table 4: Mixing proportions of the coarse aggregate interlocking concrete (kg/m^3).

No.	Cement	Water	Sand	Base stone	Add stone	Water-reducing agent
PT-0	493.3	222	736	1428.6	0	2.22
PT-5	493.3	222	736	1428.6	509	2.22
PT-10	493.3	222	736	1428.6	1018	2.22
PT-15	493.3	222	736	1428.6	1527	2.22
PT-20	493.3	222	736	1428.6	2036	2.22
PT-25	493.3	222	736	1428.6	2545	2.22

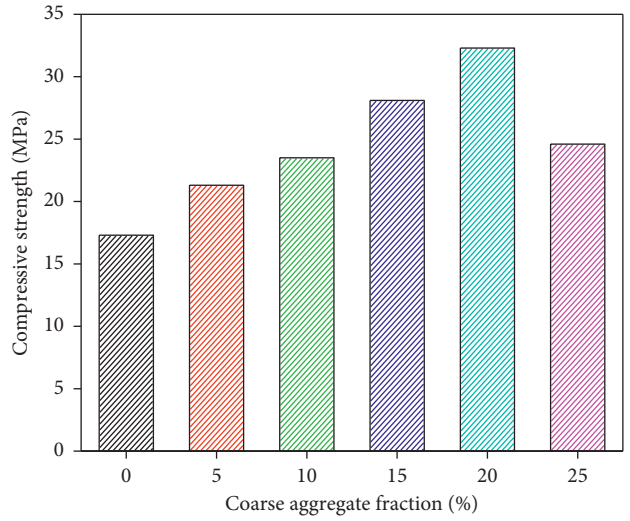

Figure 1: Compressive strength of coarse aggregate interlocking concrete subjected to different increasing amounts of coarse aggregates.

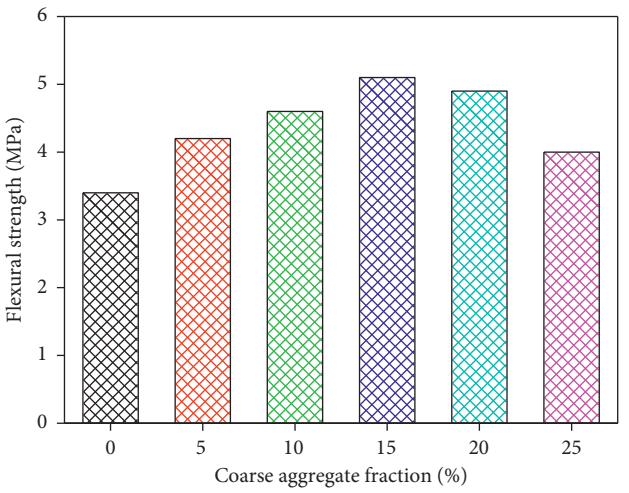

Figure 2: Flexural strength of coarse aggregate interlocking concrete subjected to different increasing amounts of coarse aggregates.

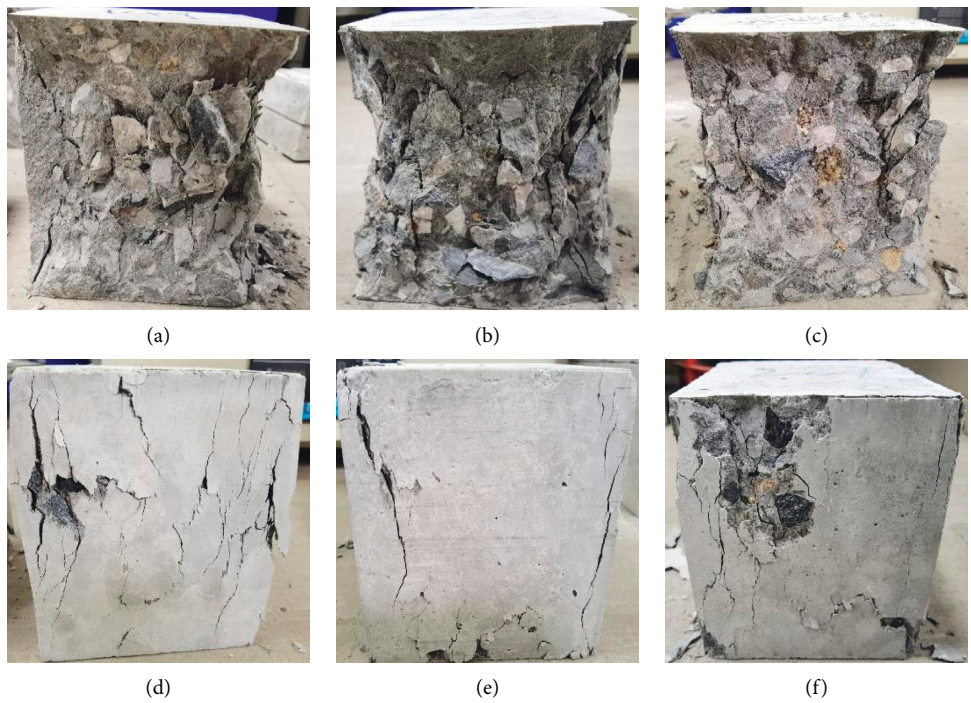

Figure 3: Failure mode of the coarse aggregate interlocking concrete subjected to different increasing amounts of coarse aggregates under compressive load. (a) PT-0. (b) PT-5. (c) PT-10. (d) PI5. (e) PT-20. (f) PT-25.

3.3.3. Test of Fracture Toughness of the Coarse Aggregate Interlocking Concrete. A notched three-point bending beam was used to determine the fracture toughness of coarse aggregate interlocking concrete. For crack generation, the specimen is made to produce cracks by cutting on the side of the specimen. The slit width is controlled at 3 mm ± 1 mm, the slit length is controlled at 80 mm ± 2 mm, and the angle between the joint surface and the specimen is $90^{\circ} \pm 0.5^{\circ}$ according to GB/T50081-2019 [29]. The size of the experimentally produced specimen is 100 mm × 100 mm × 400 mm (108 pieces).

3.3.4. Mercury Intrusion Porosimetry (MIP) Analysis. Mercury intrusion porosimetry (MIP) is the most common method used to study the pore properties of cement-based materials. This method is relatively straightforward and generally yields reproducible pore size distributions. The significant characteristic parameters, such as the total pore diameter, total porosity, and theoretical pore diameter, can be deduced from these pore size distributions. With increasing pressure, mercury is pressed into the pore structures of concrete samples. After the mercury fills the samples, the relationship between the intrusion pressure and the pore radius can be obtained. The fine particles of concrete (5 groups and 6 solid samples in each group) were subjected to mercury intrusion test analysis.

4. Results and Discussion

4.1. Experimental Values of Mechanical Characteristics of Coarse Aggregate Interlocking Concrete. Figures 1 and 2 show the experimental results of compressive and flexural strength of coarse aggregate interlocking concrete. The results show the following: (1) The macroscopic mechanical strength increases as the volume rate of the coarse aggregate increases. (2) When the volume fraction of the external coarse aggregate is 0%–20%, the strength increases with the increase in the aggregate replacement rate. When the volume rate of coarse aggregate is 15%~20%, the compressive and flexural strengths reach the maximum values, which are increased by 40% and 36%, respectively. (3) However, when

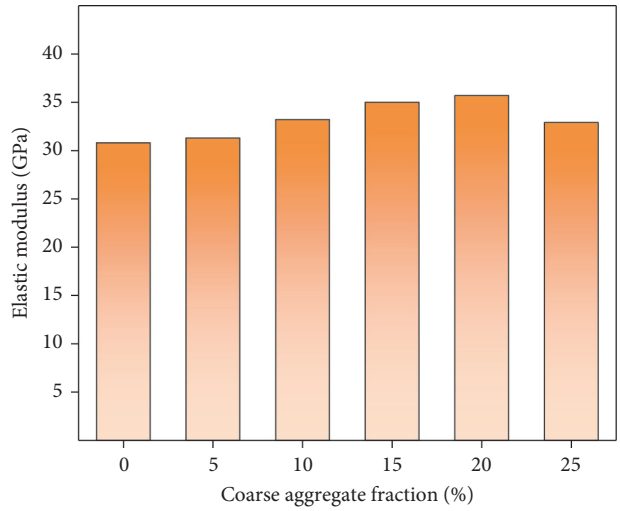

Figure 4: Elastic modulus of the coarse aggregate interlocking concrete subjected to different increasing amounts of coarse aggregates.

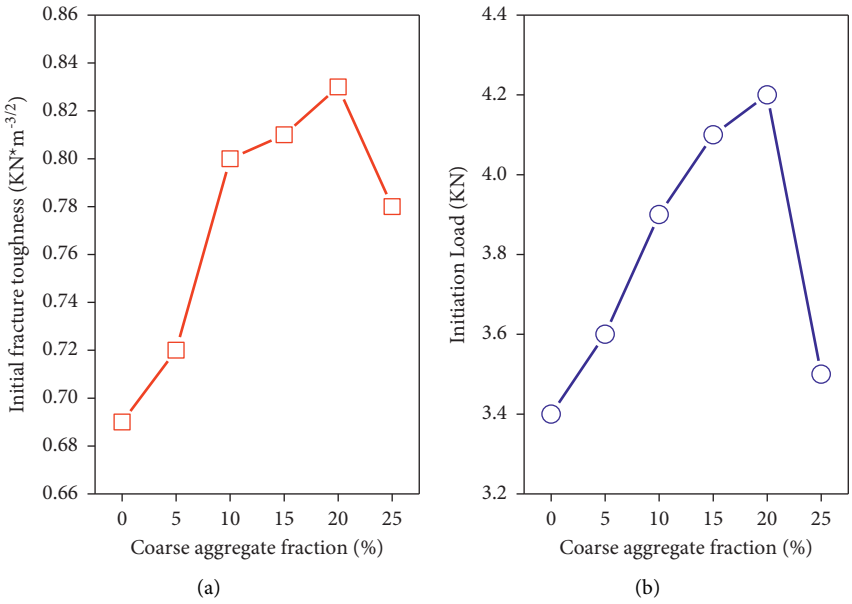

Figure 5: Initiation load and initial fracture toughness of the coarse aggregate interlocking concrete.

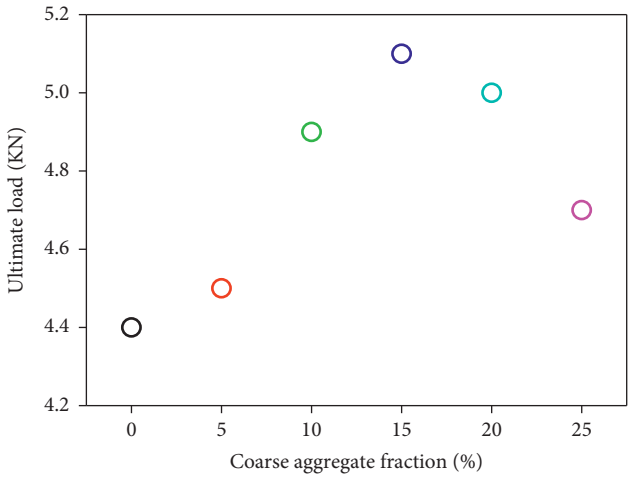

Figure 6: Ultimate load of the coarse aggregate interlocking concrete.

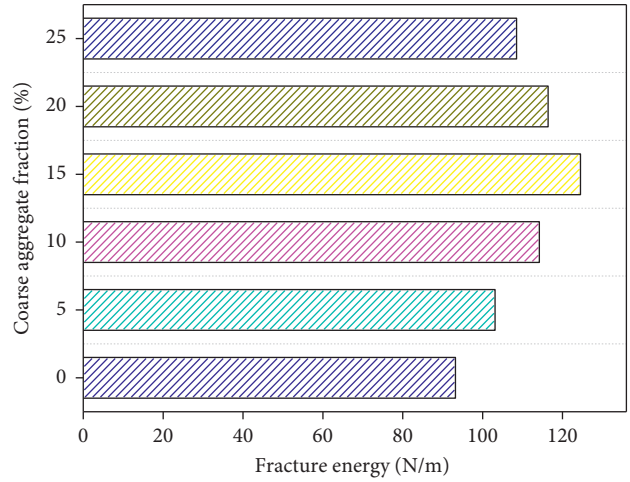

Figure 7: Fracture energy of the coarse aggregate interlocking concrete.

the volume rate of the coarse aggregate is 25%, the macromechanical properties are significantly decreased. This is because too much coarse aggregate in the concrete makes compaction difficult, which reduces the mechanical strength. However, due to the interlocking effect between the aggregates, the final mechanical strength is still higher than the reference value.

In addition, the comparative analysis of the interface morphology subjected to compression fracture is shown in Figure 3. The results show the following: (1) The increase in the volume ratio of the coarse aggregate promotes the formation of the spatial distribution of the mutual embedment and occlusion of aggregates during the concrete hydration process. (2) The increase in coarse aggregate also reduces the distribution probability of through cracks under load. (3) When the volume ratio of coarse aggregate is 20%, there is no obvious crack in the core part of the specimen during crushing failure. Figure 4 shows the elastic modulus of the coarse aggregate interlocking concrete. 5%, 10%, 15%, and 20% of the aggregate volume increased by 3.3%, 6.6%, 13%, and 19.8% compared with the elastic modulus of the benchmark group, respectively. Subsequently, when the volume of the aggregate is 25%, the elastic modulus began to decrease. The variation and evolution are similar as the abovementioned results of strength characteristics.

4.2. Experimental Values of Fracture Characteristics of Coarse Aggregate Interlocking Concrete. Figures 5 and 6 show the results of initial fracture load, ultimate fracture load, and initial fracture toughness during fracture experiment of the coarse aggregate interlocking concrete. Compared with the benchmark concrete, with the increase in aggregate volume,

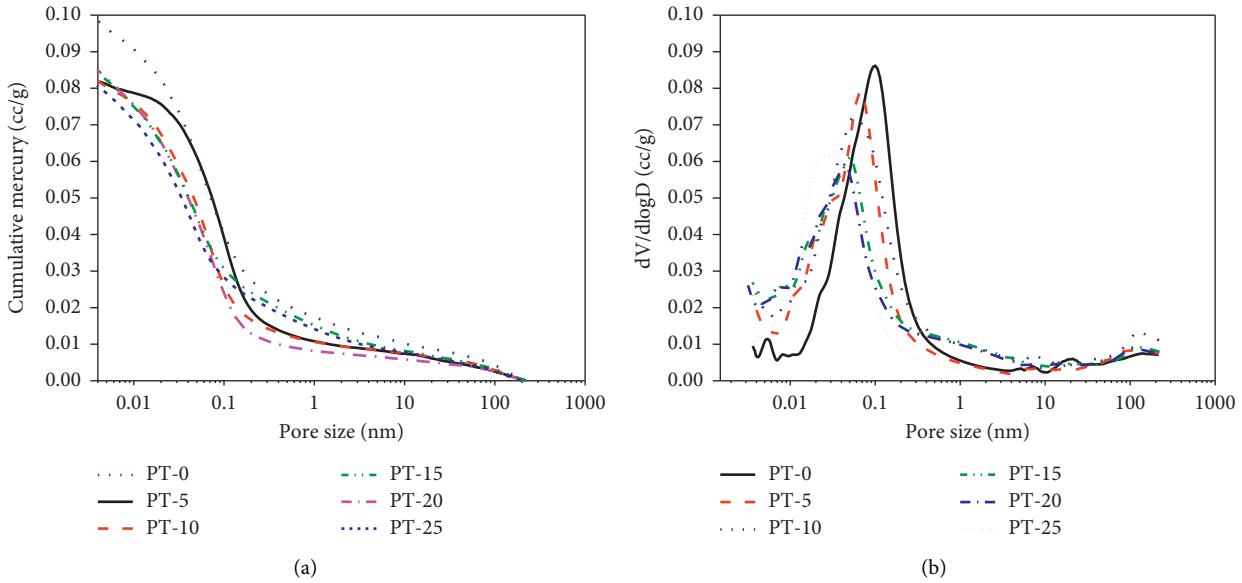

Figure 8: Pore size distribution of the coarse aggregate interlocking concrete. (a) Cumulative mercury. (b) Pore size distribution.

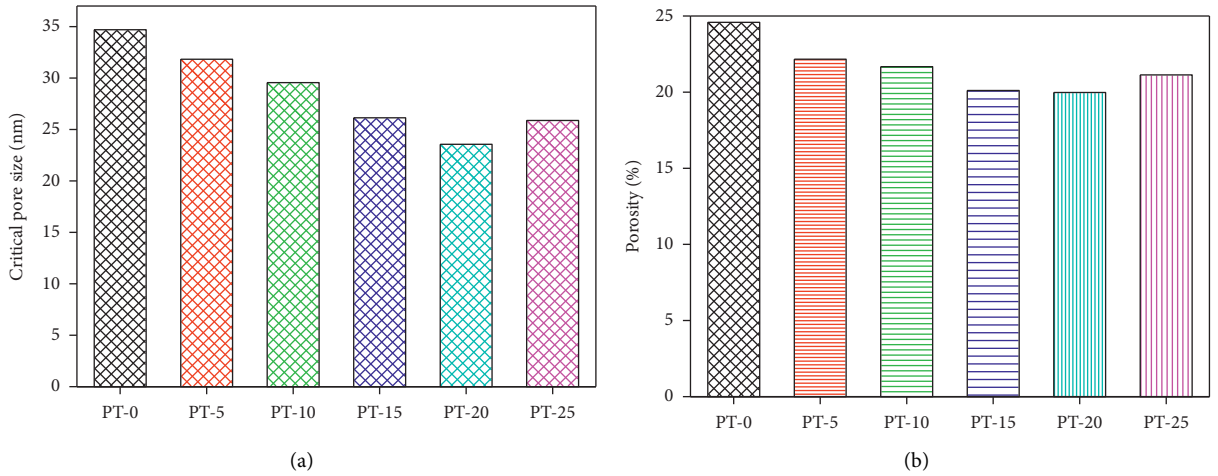

Figure 9: Pore parameters of the coarse aggregate interlocking concrete. (a) Critical pore size. (b) Porosity.

the cracking load shows an increasing trend. However, when the aggregate volume increases by 20%, the crack initiation load begins to show a downward trend. When the increase in the volume of the coarse aggregate is 0%–20%, the reason for the phenomenon of crack initiation and ultimate load enhancement is that more aggregate makes the material inside the concrete fill and compact, which improves the overall compactness of the material. When the increment reaches 20%–25%, the workability of concrete will be affected by the excessive coarse aggregate, which will reduce the cohesion of concrete and generate more internal cracks. This leads to a reduction in the initial and ultimate loads during the concrete fracture process.

According to the classical calculation equations in fracture mechanics, the test fracture energy under different coarse aggregate volume increments of the coarse aggregate interlocking concrete can be obtained and is shown in Figure 7. The results show the following: (1) When the volume increase in the coarse aggregate is 0%–20%, the fracture energy shows an increasing trend. For every 5% increase in volume, the fracture energy increases by 12.3%, 17.6%, and 19.4%, respectively. In the fracture process, a certain friction force is formed between the coarse aggregates, which indirectly increases the bite force between the coarse aggregate and the cementitious material, and the fracture energy is improved. (2) However, when the volume increase fraction of the coarse aggregate reaches 25%, the fracture energy shows a downward trend (compared to 20% aggregate volume fraction, it decreased to 25.3%). When the volume increase of the coarse aggregate reaches 25%, the bite force between the materials begins to decrease due to the decrease in the compactness, which causes the evolution of the fracture energy to show a downward trend.

4.3. Pore Size Distribution of Coarse Aggregate Interlocking Concrete. Variations in the pore size distribution of the coarse aggregate interlocking concrete obtained from the

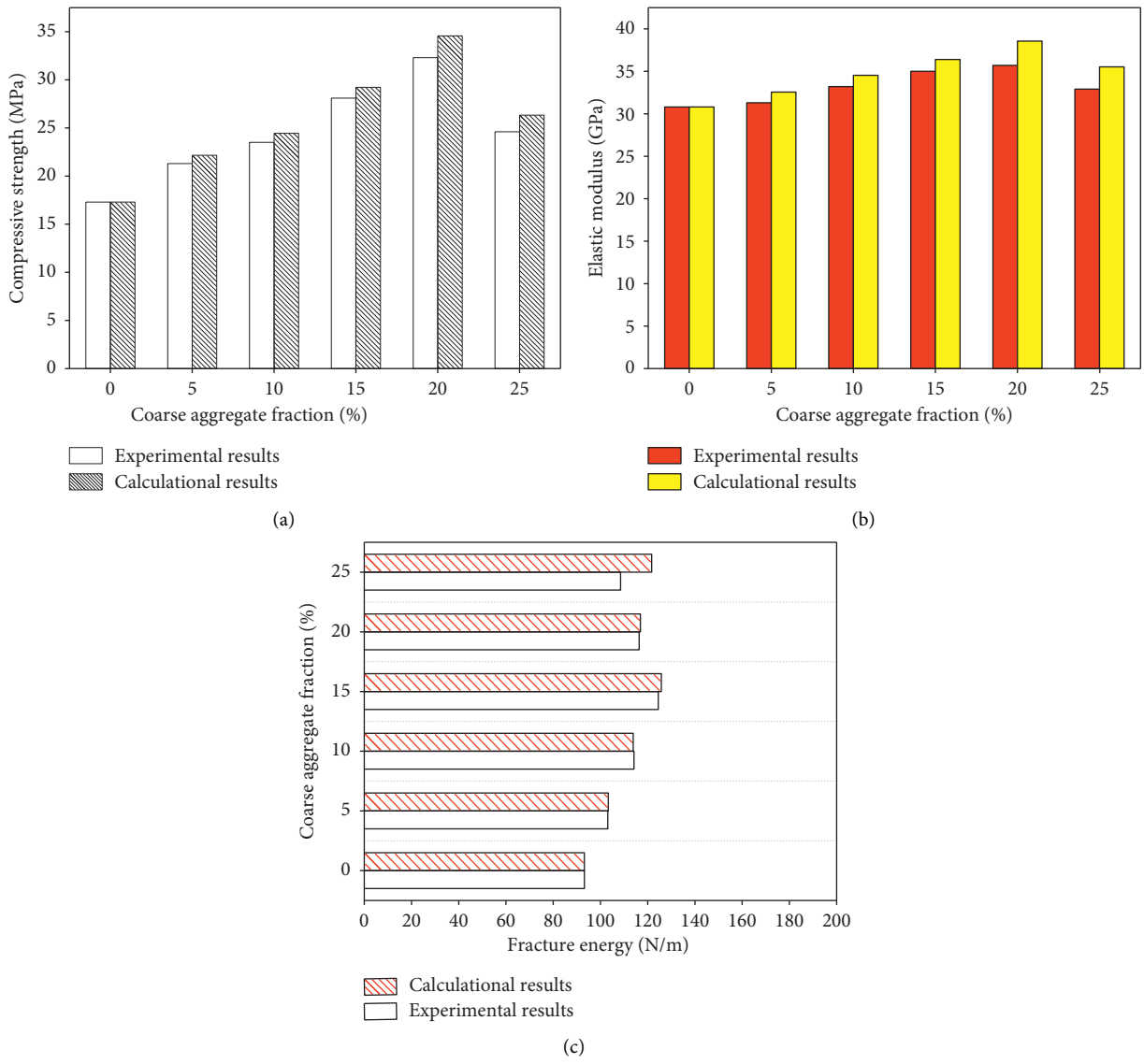

Figure 10: Comparison results of experiment and simulation calculation of the coarse aggregate interlocking concrete. (a) Compressive strength. (b) Elastic modulus. (c) Fracture energy.

pore size distribution curves based on MIP testing data are shown in Figure 8. Characteristic pore parameters such as porosity and critical pore size are shown in Figure 9. We can obtain the following: (1) With the increase in coarse aggregate volume, the porosity and critical pore size of concrete gradually decrease. (2) The appropriate increase in the volume of the coarse aggregate not only plays the role of the original strength skeleton but also improves the internal compactness of the concrete and reduces the internal pore density, which improves the ultimate strength and fracture resistance of the concrete. (3) However, the pore density increases when the volume increase of coarse aggregate is 20%~25% based on the influence of workability and insufficient wrapping of cementitious materials, in which the ultimate strength and fracture energy are significantly reduced. In summary, the coarse aggregate has an important relationship with the construction of pore structure of concrete. The change of porosity and critical pore size significantly affects the fracture toughness and ultimate strength, which provides relevant calculation parameters for the theoretical simulation calculation in this paper.

4.4. Comparison of the Fracture Characteristics Calculated by the Mesoscopic Model and Experimental Results. This section reports the results of the fracture characteristics based on the mesoscopic model (equations (8)–(10)). The comparison results and errors are shown in Figures 10 and 11. Comparing the calculation results with the experimental results, we can find the following: (1) For the simulation of compressive strength and elastic modulus, the simulation results are higher than the experimental results. However, as the volume of coarse aggregate increases, the calculation error gradually stabilizes (3~4%). The accuracy of the calculation results of higher volume increase of the coarse aggregate (>20%) is not ideal. This may be attributed to the fact that

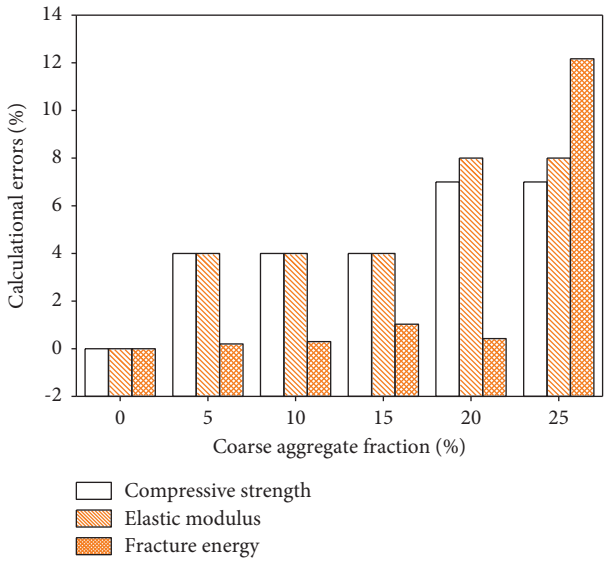

Figure 11: Calculated error values.

when the amount of coarse aggregates exceeds 20%, the distribution of aggregates inside the cement matrix is intricate and complex, which is prone to produce uneven forces on the aggregates, thus causing the calculation results to be affected and producing large fluctuations and errors. (2) For the simulation results of fracture energy, the simulation results have the same laws as the experimental results and the calculation error is small (the increase of coarse aggregate is less than 20%, and the error is 2%). The simulation results can well reflect the fracture energy development characteristics of the concrete fracture process. However, when the volume increase of coarse aggregate is large (>20%), the simulation results of fracture energy have very large errors. How to improve the accuracy of related calculation results in the future is the research content that the model still needs to consider in the future. In summary, the mesoscale multimechanical model established in this paper has certain theoretical basis and calculation accuracy.

5. Conclusions

A mesoscopic model, based on the micromechanics RVE model and fracture mechanics mechanism, was validated and applied to the experimental test for calculating the influence of coarse aggregate on fracture characteristics of the concrete. The following conclusions of this study can be drawn:

(1) Experiments and theoretical studies are conducted on the ultimate strength and fracture characteristics of concrete. The increase in coarse aggregate can significantly improve the macroscopic strength and fracture resistance of concrete within a certain range. However, as the volume increases, due to the influence of too much coarse aggregate on the working performance, the wrapping performance of the cementitious material, the pore size, and the macromechanical properties decrease (still higher than the reference value).

(2) Based on the new model, some mesoscopic mechanical models were established for describing the mechanism of coupling relationship between pore size, mechanical strength, and fracture characteristics. The proposed model was proved to be effective for evaluating mechanical response of the coarse aggregate interlocking concrete.

Data Availability

The research data used to support the findings of this study are included within the article.

Disclosure

The Key Laboratory of Transport Industry of Road Structure and Material and Foshan University is the co-first unit. Ben Li and Ying Yu are considered as the co-first authors.

Conflicts of Interest

The authors declare that they have no conflicts of interest.

Authors' Contributions

Ben Li and Ying Yu contributed equally to this work.

Acknowledgments

The authors acknowledge the financial support provided by the Science and Technology Innovation Platform of Foshan City (Grant no. 2016AG100341, Guangdong Province, China). The authors also thank the team members from ASIM Group, China, the support from Foshan Intelligent Land and Ocean Engineering Materials Engineering Technology Research and Development Center, Foshan, China.

References

[1] C. Zhang, X. Hu, T. Sercombe, Q. Li, Z. Wu, and P. Lu, "Prediction of ceramic fracture with normal distribution pertinent to grain size," *Acta Materialia*, vol. 145, pp. 41–48, 2018.

[2] R. Xu and X. Hu, "Effects of nano-grain structures and surface defects on fracture of micro-scaled polysilicon components," *Journal of the American Ceramic Society*, vol. 103, no. 6, pp. 3757–3762, 2020.

[3] B. Yuan, Y. Hu, and X. Hu, "Critical bending load of CFRP panel with shallow surface scratch determined by a tensile strength model," *Composites Science and Technology*, vol. 191, Article ID 108072, 2020.

[4] G. Sun, Y. Zhang, W. Sun, Z. Liu, and C. Wang, "Multi-scale prediction of the effective chloride diffusion coefficient of concrete," *Construction and Building Materials*, vol. 25, no. 10, pp. 3820–3831, 2011.

[5] Y. Zhou, Z. Fan, J. Du, L. Sui, and F. Xing, "Bond behavior of FRP-to-concrete interface under sulfate attack: an experimental study and modeling of bond degradation," *Construction and Building Materials*, vol. 85, pp. 9–21, 2015.

[6] T. Luping, "Engineering expression of the ClinConc model for prediction of free and total chloride ingress in submerged marine concrete," *Cement and Concrete Research*, vol. 38, no. 8-9, pp. 1092–1097, 2008.

[7] X. Han, Y. Chen, X. Hu, W. Liu, Q. Li, and S. Chen, "Granite strength and toughness from small notched three-point-bend specimens of geometry dissimilarity," *Engineering Fracture Mechanics*, vol. 216, Article ID 106482, 2019.

[8] D. R. Rilem, "Determination of the fracture energy of mortar and concrete by means of three-point bend tests on notched beams," *Materials and Structures*, vol. 18, no. 106, pp. 285–290, 1985.

[9] Z. P. Bažant, "Size effect in blunt fracture: concrete, rock, metal," *Journal of Engineering Mechanics*, vol. 110, no. 4, pp. 518–535, 1984.

[10] M. Zhang, G. Ye, and K. van Breugel, "Multiscale lattice Boltzmann-finite element modelling of chloride diffusivity in cementitious materials. Part I: Algorithms and implementation," *Mechanics Research Communications*, vol. 58, pp. 53–63, 2014.

[11] M. Zhang, G. Ye, and K. van Breugel, "Multiscale lattice Boltzmann-finite element modelling of chloride diffusivity in cementitious materials. Part II: simulation results and validation," *Mechanics Research Communications*, vol. 58, no. 28, pp. 64–72, 2014.

[12] O. Truc, J. P. Ollivier, and L. O. Nilsson, "Numerical simulation of multi-species diffusion," *Materials and Structures*, vol. 33, pp. 566–573, 2010.

[13] A. Boddy, E. Bentz, M. D. A. Thomas, and R. D. Hooton, "The University of Toronto chloride transport model: an overview and sensitivity study," *Cement and Concrete Research*, vol. 12, pp. 827–837, 2001.

[14] F. P. Glasser, J. Marchand, and E. Samson, "Durability of concrete-degradation phenomena involving detrimental chemical reactions," *Cement and Concrete Research*, vol. 11, no. 38, pp. 226–246, 2008.

[15] R. A. Cook and K. C. Hover, "Mercury intrusion porosimetry of cement-based materials and associated correction factors," *Construction and Building Materials*, vol. 4, no. 7, pp. 231–240, 2007.

[16] J. Kaufmann, F. Winnefeld, and R. Zurbriggen, "Polymer dispersions and their interaction with mortar constituents and ceramic tile surfaces studied by zeta-potential measurements and atomic force microscopy," *Cement and Concrete Composites*, vol. 34, no. 5, pp. 604–611, 2012.

[17] M. V Tran and B. Stitmannaithum, "Chloride penetration into concrete using various cement types under flexural cyclical load and tidal environment," *The IES Journal Part A: Civil & Structural Engineering*, vol. 13, pp. 201–214, 2015.

[18] A. Hillerborg, "Results of three comparative test series for determining the fracture energyG F of concrete," *Materials and Structures*, vol. 18, no. 5, pp. 407–413, 1985.

[19] D. G. Zollinger, T. Tang, and R. H. Yoo, "Fracture toughness of concrete at early ages," *ACI Materials Journal*, vol. 90, no. 5, pp. 463–471, 1993.

[20] S. Dehghanpoor Abyaneh, H. S. Wong, and N. R. Buenfeld, "Modelling the diffusivity of mortar and concrete using a three-dimensional mesostructure with several aggregate shapes," *Computational Materials Science*, vol. 78, no. 5, pp. 63–73, 2013.

[21] K. M. A. Sohel, K. Al-Jabri, M. H. Zhang, and J. Y. R. Liew, "Flexural fatigue behavior of ultra-lightweight cement composite and high strength lightweight aggregate concrete," *Construction and Building Materials*, vol. 173, pp. 90–100, 2018.

[22] S. Pyo, S. Y. Abate, and H.-K. Kim, "Abrasion resistance of ultra high performance concrete incorporating coarser aggregate," *Construction and Building Materials*, vol. 165, no. 165, pp. 11–16, 2018.

[23] M. Shafieifar, M. Farzad, and A. Azizinamini, "Experimental and numerical study on mechanical properties of ultra high performance concrete (UHPC)," *Construction and Building Materials*, vol. 156, no. 156, pp. 402–411, 2017.

[24] M. K. Lee and B. I. G. Barr, "An overview of the fatigue behaviour of plain and fibre reinforced concrete," *Cement and Concrete Composites*, vol. 26, no. 4, pp. 299–305, 2004.

[25] S. Seitl, V. Bílek, Z. Keršner, and J. Veselý, "Cement based composites for thin building elements: fracture and fatigue parameters," *Procedia Engineering*, vol. 2, no. 1, pp. 911–916, 2010.

[26] J. Wang, P. A. M. Basheer, S. V. Nanukuttan, A. E. Long, and Y. Bai, "Influence of service loading and the resulting microcracks on chloride resistance of concrete," *Construction and Building Materials*, vol. 108, pp. 56–66, 2016.

[27] V. Picandet, A. Khelidj, and G. Bastian, "Effect of axial compressive damage on gas permeability of ordinary and high-performance concrete," *Cement and Concrete Research*, vol. 31, no. 11, pp. 1525–1532, 2001.

[28] *JTG 3420-2020*, Test Methods of Concrete and Cement for Highway Engineering, Beijing, 2020.

[29] *GB/T 50081-2019, Standard for Test Method of Mechanical Properties on Ordinary concrete*, Beijing, 2019.